中國工程學刊第十卷第三期（民國七十六年）
Journal of the Chinese Institute of Engineers. Vol. 10, No. 3, pp. 241-250 (1987)



# MODELING AND OPTIMAL CONTROL OF A LIGHTWEIGHT BRACING MANIPULATOR

Ya-Chien Chung and Shui-Shong Lu

*Department of Mechanical Engineering*
*National Taiwan University*
*Taipei, Taiwan 10764, R.O.C.*

Wayne J. Book

*School of Mechanical Engineering*
*Georgia Institute of Technology*
*Atlanta, Georgia 30332, U.S.A.*

***Key Words***: bracing manipulator, robotics.

## ABSTRACT

Bracing strategy can improve the stiffness of a lightweight manipulator. A lightweight bracing manipulator provides better manuverability in gross motions and higher precision in small motions. In order to maintain these advantages, the structure and dynamics of these types of manipulators become more complicated. In this paper, the dynamic model, which includes gravitational effects and an optimal regulator with prescribed relative stability, is developed. The influence of the modeling uncertainties on the controlled system is considered.

# 輕量支撐機械手的動態模式之建立與控制

鍾雅健　　呂秀雄

國立臺灣大學機械研究所

Wayne J. Book

美國喬治亞理工學院機械工程系

## 摘　　要

輕量機械手比一般之機械手具有更好的機動性，但卻具備較差之剛性。新發展的支撐原理可以加強輕量機械手結構之剛性。本文將針對此綜合輕量與支撐二優點之輕量支撐機械手進行研究。本文中之輕量支撐機械手，爲了保有以上之二優點，結構變得格外複雜。在尋求其動態方程式時之困難，除了面對一個封閉之四連桿之外，還必須考慮一些輕量桿件之振動及支撐點之邊界條件。本文將應用 Hamilton 氏原理及模式叠代法，建立一包括重力效應的動態模式。然後再應用此動態模式及一可設定相對穩定度的最佳控制方法，進行結構減振控制的分析。

## INTRODUCTION

A manipulator needs gross motions to cover the entire task space and very precise motions to accomplish a specific job. For the gross motions, it is definitely an advantage if a lightweight manipulator is used. The lightweight manipulator has many advantages such as higher speed, smaller actuators, lower energy consumption, lower cost, and safer working conditions, but it also has many shortcomings such as lower stiffness, larger vibration, and unnecessary collision induction.

On the other hand, for precise motion, a manipulator requires higher stiffness for the structure. Obviously, the link structure of a lightweight manipulator becomes the major source of structural compliance. There is a conflict improving between the gross motions and the precise motions. There have been many investigations considering this problem. Most of them have tried to damp out the unnecessary vibration by applying control algorithms to the lightweight structure [6, 7, 10] or using damping material on the structure [1]. A bracing strategy may be applied to increase the stiffness of the lightweight structure. In order to write better, people would brace their wrists on a surface such as a table. This is the basic concept of a bracing manipulator. The bracing strategy was described by Book et al. in 1984 [8]. Asada and West [4] applied a similar strategy on a grinding manipulator to improve the dynamic characteristics of the structure in grinding operations.

In order to maintain the advantages of the lightweight bracing manipulator, the actuators of the manipulator should be located at a position as low as possible. An actuating link is required to transfer the necessary torque. The structure of the lightweight bracing manipulator is basically the same structure reported by Wilson [15] and Holden [12]. The lower section of the structure is a four-bar linkage. The dynamics of the structure becomes complicated due to the bracing condition and the flexible elements.

The structural dynamics, including the rigid body motions and the flexible vibrations, can be modeled by using Euler-Newton's method [11], Hamilton's principle [14], Kane's method [13], or numerical methods such as the finite element method [5]. Constrained conditions for the closed four-bar linkage and the boundary condition at the bracing point make the modeling work more complicated. To avoid the necessity of constrained conditions, a dynamic model of the lightweight bracing manipulator is developed in this paper. In addition to using Hamilton's principle, the modes superposition method is used to simplify the modeling work, and an appropriate admissible function in the modes superposition method is used to satisfy the boundary condition of bracing.

The lightweight bracing manipulator is an elastic structure. The highest natural frequency needed to be controlled is related to the number of assumed modes. For implementation, the effect of the control depends on the spectrum and the maximum output of the actuator. As a matter of fact, the more relative stability the closed loop system needs, the larger the output required of the actuator. For flexible structures, discontinuous actuation should be avoided, therefore, an optimal control with a prescribed relative stability is definitely helpful for this system. In this paper, the algorithm of the linear quadratic optimal control with prescribed relative stability is applied to control the flexible manipulator at any nominal angular configuration within the working range.

## MODELING OF THE LIGHTWEIGHT BRACING MANIPULATOR

The schematic diagram of the lightweight manipulator is shown in Fig. 1. Assume that the motion of the whole structure is in a vertical plane. Any flexible part is treated as a Euler-Bernoulli beam, i.e., the deflection is pure bending in the plane of the manipulator.

The lower section of the whole structure is a four-bar linkage, consisting of a section of the upper link, the lower connecting link, the lower link and the actuating link, as noted in Fig. 1. The former two are reinforced structures that can be reasonably assumed rigid in the analysis. The lower link and upper link are considered flexible. The actuating link is much less stiff than the lower

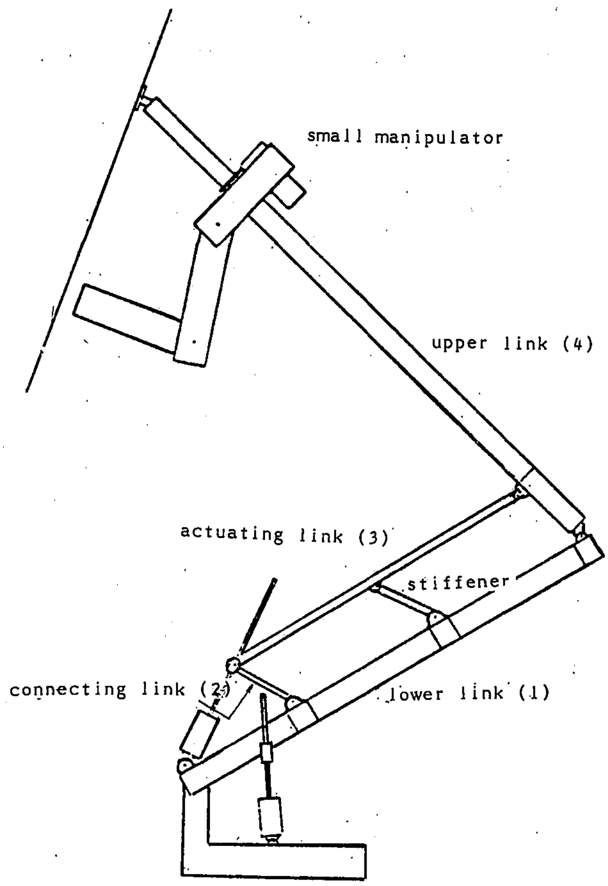


Fig. 1. Schematic diagram of the lightweight bracing manipulator.

link in bending modes, so that the actuating link has a small effect on the natural frequencies caused by the lower link. Assume that the actuating link deflects coincidentally with the lower link. This assumption is more reasonable when there is a stiffener in the four-bar linkage as shown in Fig. 1.

To simplify the analysis, further assumptions are: the lower link and the actuating link have the same length; there is no interactive force between the large manipulator and the small manipulator structures; the small manipulator is treated as a lumped mass; and all elastic deflections are relatively small. Using the above assumptions, the physical model and the coordinates for the mathematical model can be constructed as shown in Fig. 2. $X$ and $Y$ are the axes of the fixed coordinate system. $X_1$, $Y_1$ and $X_2$, $Y_2$ are the local coordinates moving with the structure motion. $X_1$ is defined to be tangent of the lower link at the origin of the fixed coordinate system. $X_2$ is defined along the rigid part of the upper link. $u_1$ and $u_2$ are the perpendicular distances from the points on the structure to $X_1$ and $X_2$ axes respectively. $\theta_1$ is the angle between $X_1$ and $X$. $\theta_2$ is the angle between $X_2$ and $X_1$. $\tau_1$ is the equivalent torque applied on the $\theta_1$ dimension and $\tau_2$ is the torque for the $\theta_2$ dimension.

### Kinetic energy

The kinetic energy of the whole structure is:

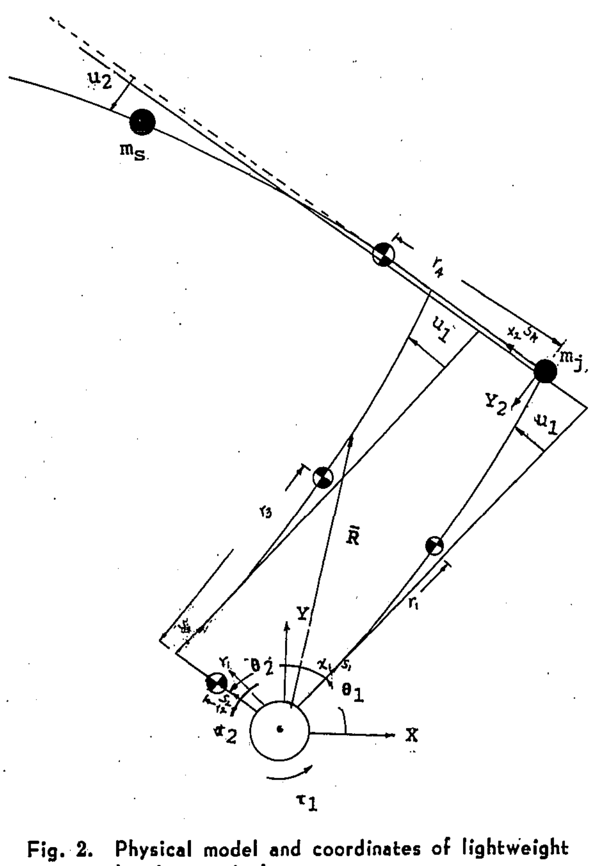

Fig. 2. Physical model and coordinates of lightweight bracing manipulator.

$$K=\frac{1}{2}\int\rho_1\dot{\bar{R}}\cdot\dot{\bar{R}}dz_1+\frac{1}{2}\int\rho_2\dot{\bar{R}}\cdot\dot{\bar{R}}dz_2$$
$$+\frac{1}{2}\int\rho_3\dot{\bar{R}}\cdot\dot{\bar{R}}dz_3+\frac{1}{2}\int\rho_4\dot{\bar{R}}\cdot\dot{\bar{R}}dz_4$$
$$+\frac{1}{2}m_s|\dot{\bar{R}}\cdot\dot{\bar{R}}|\text{ (at a small manipulator position)}$$
$$+\frac{1}{2}m_j|\dot{\bar{R}}\cdot\dot{\bar{R}}|\text{ (at the end of lower link).} \quad (1)$$

In Eq. (1), $\rho_i$'s are the masses per unit length of the links, and the subscripts 1, 2, 3, and 4 are the lower link, the connecting link, the actuating link, and the upper link, respectively. The variables $z_i$'s are coordinates along each link as shown in Fig. 2. $\bar{R}$ is the position vector of any point on the structure. A dot over a variable denotes its time derivative and a dot between two vectors indicates their inner product.

### Potential energy

Let $m_i$ be the respective masses of $i$th link and $r_i$ be the respective positions of the center of mass of $i$th link as shown in Fig. 2. $EI_i$'s are the respective bending stiffnesses of each flexible link, where $E$ is the modulus of elasticity and $I$ is the moment of the link cross sectional area. The total potential energy of the lightweight bracing manipulator, consisting of the gravitational potential and the bending strain energy can be written as

$$V=m_1gr_1s_1-m_2gr_2s_{12}+m_3g[r_3s_1+\ell_2s_{12}]$$
$$+m_3g(r_4s_{12}+\ell_1s_1)+m_jg\ell_1s_1$$
$$+m_sg[\ell_1s_1+\ell_ss_{12}]$$
$$+\frac{1}{2}(EI_1+EI_3)\int_0^{\ell_1}u_1''^2dz_1$$
$$+\frac{1}{2}EI_4\int_0^{\ell_4}u_2''^2dz_4 \quad (2)$$

where $s_1=\sin\theta_1$ an $s_{12}=\sin(\theta_1+\theta_2)$.

### Work done by external forces

There are two external torques, $\tau_1$ and $\tau_2$; each is applied to $\theta_1$ and $\theta_2$ dimensions respectively. In the braced case, the reactive force at the end effector is also an external force of the structure. To simplify the analysis, the reactive force at the end effector is neglected. The work done by $\tau_1$ and $\tau_2$ is:

$$\Delta A'=\tau_1\Delta\theta_1+\tau_2\Delta\theta_2. \quad (3)$$

### Hamilton's principle

The system dynamics must satisfy Hamilton's principle, i. e.,

$$\int_0^t\delta(K-V+A')dt=0. \quad (4)$$

Using Eqs. (1)-(3), and integration by parts, $\delta\dot{\theta}_1$, $\delta\dot{\theta}_2$, $\delta\dot{u}_1$, and $\delta\dot{u}_2$ in the equation can be changed into $\delta\theta_1$, $\delta\theta_2$, $\delta u_1$, and $\delta u_2$. Because the four coordinates, $\theta_1$, $\theta_2$ $u_1$, and $u_2$, are independent, one will be able to obtain four equations from this equation. These are two ordinary differential equations for rigid body motions, and two partial differential equations for the motions of flexural elements.

### Modes superposition method

The modes superposition method will be applied to simplify the analysis by assuming $u_1$ and $u_2$ to be:

$$u_1(z_1,\ t)=\sum_{i=1}^{N}\phi_{1i}(z_1)q_{1i}(t) \tag{5}$$

$$u_2(z_4,\ t)=\sum_{i=1}^{N'}\phi_{2i}(z_4)q_{2i}(t). \tag{6}$$

$\phi_{1i}$ and $\phi_{2i}$ are the admissible functions which must satisfy the geometrical boundary conditions. $q_{1i}$ and $q_{2i}$ are the generalized coordinates of $u_1$ and $u_2$. For the lower link, $\phi_{1i}$ is the mode shape of the clamped-free beam. For the upper link, the admissible functions for the non-braced case, $\phi_{2i}$, are chosen as the same as those for the lower link case. For the braced case, the mode shape of a clamped-pinned beam is chosen to be the admissible function for the upper link. It is assumed that $N=2$ and $N'=2$. All higher order terms of $u_1$ and $u_2$ are neglected. Equation (4) then becomes six coupled ordinary equations which can be linearized by neglecting all nonlinear terms by assuming that the manipulator moves slightly around a nominal angular position. Then these equations can be represented in state space form with a system of order twelve. That is

$$\dot{\boldsymbol{x}}=\boldsymbol{A}\boldsymbol{x}+\boldsymbol{B}\boldsymbol{u}. \tag{7}$$

The derivation of the equations and the matrices $\boldsymbol{A}_{12\times12}$, $\boldsymbol{B}_{12\times2}$ and $\boldsymbol{u}_{2\times1}$ in the equation are detailed in Ref. [9]. $\boldsymbol{x}$ is the state variable vector, i.e.,

$$\boldsymbol{x}=[q_{11},\ q_{12},\ q_{21},\ q_{22},\ \theta_1',\ \theta_2',\ \dot{q}_{11},\ \dot{q}_{12},\ \dot{q}_{21},\ \dot{q}_{22},\ \dot{\theta}_1',\ \dot{\theta}_2'].$$

## LINEAR OPTIMAL REGULATOR WITH PRESCRIBED RELATIVE STABILITY

By assuming that the manipulator moves slightly about the nominal angular position, a linear time-invariant model was found as described in the second section. Although there are only two external torques on the $\theta_1$ and $\theta_2$ dimensions and no external forces on the flexible mode dimension, the coupling of the inertia terms exist between each flexible mode and the rigid body mode. Therefore, the linearized model is completely controllable with state feedback control. The linear quadratic optimal control algorithm with a prescribed relative stability is used to design the regulator. This design assumes that the actuators are not saturated at any time and that the system is completely observable.

The objective of this modified regulator is to design optimal control which has all real parts of the closed loop eigenvalues less than a value $(-a)$. This technique was first studied by Anderson and Moore [2] and it is thought to be more suitable for the flexible system than the original control technique.

The modification starts with the definitions

$$\boldsymbol{x}'(t)=e^{at}\boldsymbol{x}(t) \tag{8}$$

$$\boldsymbol{u}'(t)=e^{at}\boldsymbol{u}(t). \tag{9}$$

From these definitions, $\boldsymbol{x}(t)$ and $\boldsymbol{u}(t)$ will be stable $\{\boldsymbol{x}(t)$ or $u(t)\to0$ when $t\to\infty\}$ only if $\boldsymbol{x}(t)$ and $\boldsymbol{u}(t)$ decay faster than $e^{-at}$. This is equivalent to requiring the closed loop system having a degree of stability of at least $a$.

The function inside the integral sign of the cost function can be modified to be

$$\boldsymbol{u}'^T\boldsymbol{R}\boldsymbol{u}'+\boldsymbol{x}'^T\boldsymbol{Q}\boldsymbol{x}'=e^{2at}(\boldsymbol{u}^T\boldsymbol{R}\boldsymbol{u}+\boldsymbol{x}^T\boldsymbol{Q}\boldsymbol{x}). \tag{10}$$

Instead of solving Eq. (7), we solve the modified system as follows:

$$\dot{\boldsymbol{x}}'=(\boldsymbol{A}+a\boldsymbol{I})\boldsymbol{x}'+\boldsymbol{B}\boldsymbol{u}'. \tag{11}$$

The modified performance index is

$$\int_0^t(\boldsymbol{x}'^T\boldsymbol{Q}\boldsymbol{x}'+\boldsymbol{u}'^T\boldsymbol{R}\boldsymbol{u}')dt. \tag{12}$$

The control $u(t)$ is the linear state function, i.e.,

$$\boldsymbol{u}'=-\boldsymbol{F}\boldsymbol{x}' \tag{13}$$

and the matrix $\boldsymbol{F}$ can be evaluated with

$$\boldsymbol{F}=\boldsymbol{R}^{-1}\boldsymbol{B}^T\boldsymbol{P} \tag{14}$$

where $\boldsymbol{P}$ must satisfy the Riccati's equation, which is

$$\boldsymbol{P}\boldsymbol{A}+\boldsymbol{A}^T\boldsymbol{P}+\boldsymbol{Q}-\boldsymbol{P}\boldsymbol{B}\boldsymbol{R}^{-1}\boldsymbol{B}^T\boldsymbol{P}=0. \tag{15}$$

Newton's numerical method [3] can be used to find the steady state solution of Eq. (15). Equation (14) is then used to obtain the feedback gain matrix, $\boldsymbol{F}$.

Substituting Eqs.(8) and (9) into Eq. (13), we obtain

$$\boldsymbol{u}=e^{-at}\boldsymbol{u}'\doteq-e^{at}\boldsymbol{F}(e^{at}\boldsymbol{x})=-\boldsymbol{F}\boldsymbol{x} \tag{16}$$

the optimal feedback gain of the modified regulator problem can be found from the control law of the original problem and the closed loop system of the original problem will have a degree of stability of $a$ at least.

**Simulation**

Choose the data of the designed lightweight bracing manipulator to be as in appendix A. For the non-braced case, use the diagonal weighting matrices shown in appendix B, and consider the prescribed relative stability with $a=3$, the nominal angular position is assumed to be $\theta_1=17°$; $\theta_2=116°$. Each element in the weighting matrices can be set to larger values when a smaller response of the respective state is needed. Applying the equations described in the third section, the feedback gains of the regulator and the eigenvalues of the closed loop system are found and shown in appendix B. For the braced case, use the same weighting matrices as in appendix B, and consider the prescribed relative stability with $a=3$, the feedback gains of the regulator and the eigenvalues of the closed loop system can be found and are shown in appendix B.

Using the feedback gains of the nonbraced case to control the linearized nonbraced model, the control is activated after an impulse signal is applied on $\theta_1$ dimension. The time responses of state variables are evaluated by the Runge-Kutta method and shown in Figs. 3 through 5. Similarly, applying the control gains found in appendix B for the braced case, the time responses of state variables are shown in Figs. 6 through 8.

Figures 4 and 7 show that the links of manipulator vibrate in a smaller displacement while an impulse of torque under the braced case is applied, so that the manipulator has higher stiffness while it is braced.

## THE EFFECT OF BRACING REACTIVE FORCE

From the linearized lightweight bracing manipulator's model, good results could be expected. Actually, there are many uncertainties in the system, which are not shown in the controlled mathematical model because of the assumptions made or because of simplification of the expressions. These uncertainties, such as nonlinear dynamic terms and the reactive force on the bracing foot will be considered in this section to check the influences on the developed linear optimal regulator.

Under bracing conditions, keeping the bracing foot from losing contact with the working surface is definitely necessary. Once the bracing foot loses contact with the surface, not only there is no bracing, but there is a higher possibility of

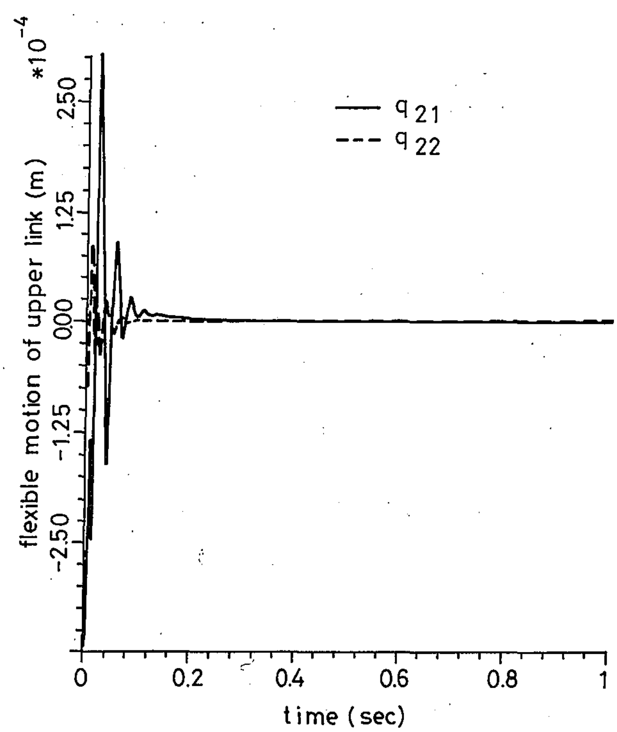


Fig. 3. Optimal control of lightweight bracing manipulator with prescribed relative stability, nonbraced case.

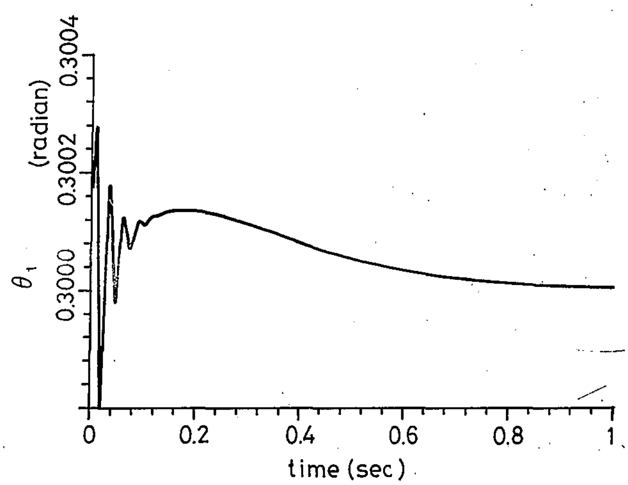


Fig. 4. Optimal control of lightweight bracing manipulator with prescribed relative stability, nonbraced case.

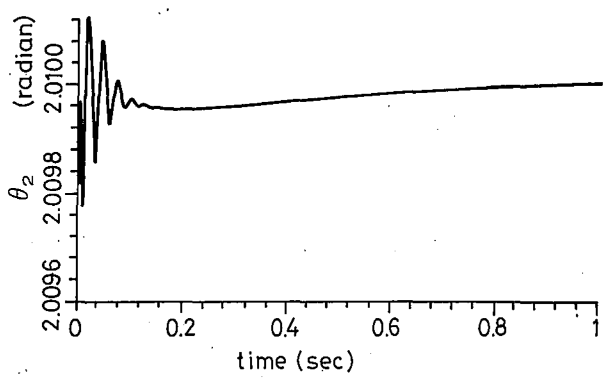


Fig. 5. Optimal control of lightweight bracing manipulator with prescribed relative stability, nonbraced case.

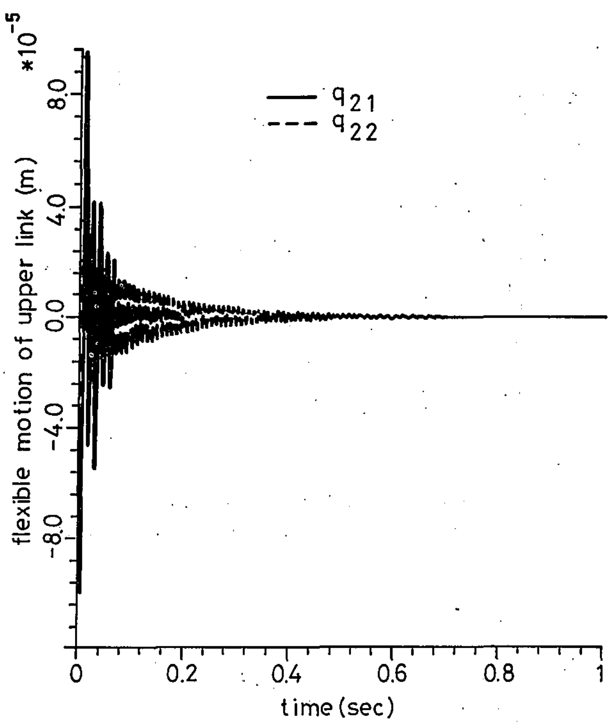


Fig. 6. Optimal control of lightweight bracing manipulator with prescribed relative stability, braced case.

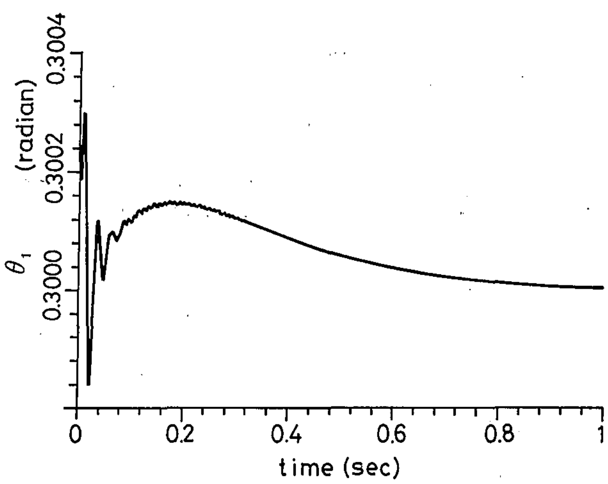


Fig. 7. Optimal control of lightweight bracing manipulator with prescribed relative stability, braced case.

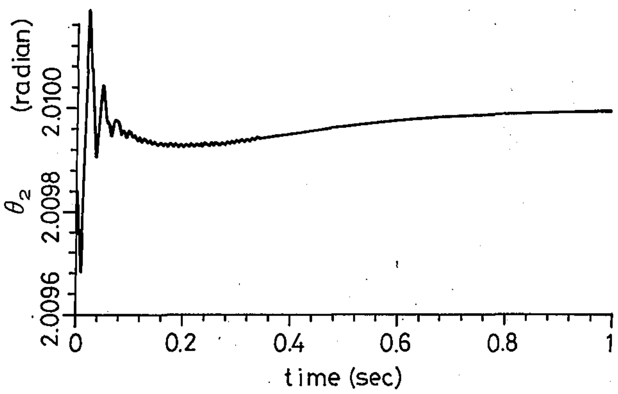


Fig. 8. Optimal control of lightweight bracing manipulator with prescribed relative stability, braced case.

collision. Therefore, the bracing point needs enough friction to prevent detachment from the surface and sliding along the surface.

To prevent sliding from happening, the critical condition is that reaction force, $R$, between the bracing foot and the working surface should be equal to the shear force, $S$, at the end section of the upper link, as shown in Fig. 9. Assume that the longitudinal force in the beam is much less than the shear force. The reaction force normal to the working surface is

$$R_N = S\cos\left(\theta_1+\theta_2+\frac{\pi}{2}-\theta_w\right) \tag{17}$$

where $\theta_w$ is the angle between the normal to the working surface and the fixed $X$-axis. The component of the reaction force parallel to the working surface must be

$$R_P = S\sin\left(\theta_1+\theta_2+\frac{\pi}{2}-\theta_w\right). \tag{18}$$

From Eqs. (17) and (18), the coefficient of friction must be

$$\mu = \frac{R_P}{R_N} > \cot(\theta_1+\theta_2-\theta_w) \tag{19}$$

so that there is no sliding between the bracing foot and the working surface.

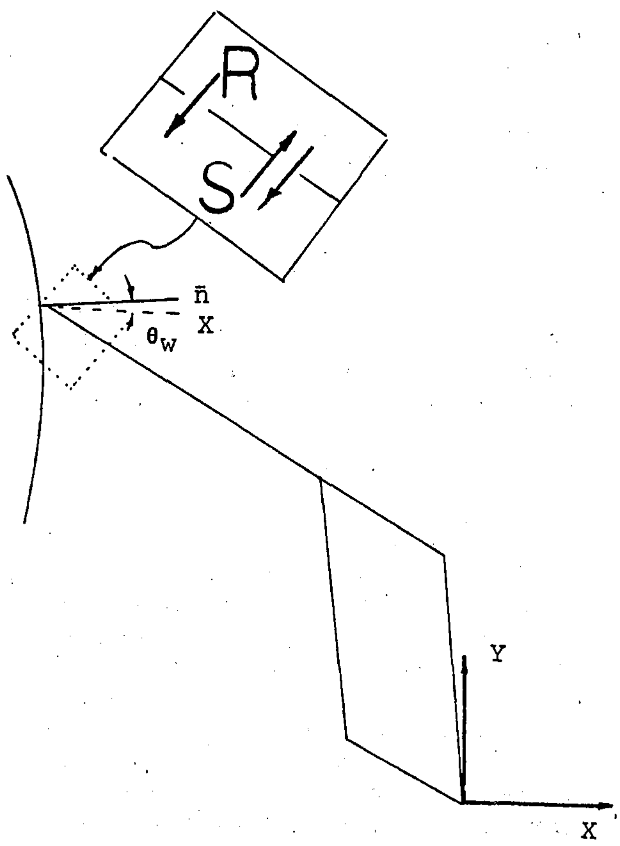


Fig. 9. Microview of bracing point.

In order to prevent detachment of the bracing foot, the direction of the reactive force must always be kept towards the working surface. If the reaction force reverses, the bracing foot will have a tendency to leave the working surface. Practically, an initial static force could be applied on the structure to improve the contact situation.

The reactive force on the bracing foot is caused by two sources, one is the deviation of the horizontal levels between the two ends of the upper link and the other is the dynamic deformation of the link. The deviation was assumed to be zero in the assumed clamped-pinned modes. As a matter of fact, this deviation is not always zero. When $\theta_1'$ and $\theta_2'$ or the displacement of the endpoint of the lower link, $u$, exists, the deviation is given by

$$\epsilon=(\ell_4-\ell_e)(\theta_1'+\theta_2')+u_{1E}c2. \tag{20}$$

Applying the relation between the free end force and the deformation of the clamped free beam to cause the deviation of the ends of the upper link, the shear force must be

$$R_1=\frac{-3\epsilon EI_4}{(\ell_4-\ell_e)^3}. \tag{21}$$

Defining the directions of the forces, $R$ and $S$, in Fig. 9 to be positive, the force caused by the dynamic deflection is

$$R_2=-EI_4\frac{\delta^3 u_2}{\delta^3 s}\bigg|_{z_4=\ell_4}. \tag{22}$$

So that the total shear, or the total reaction force against the manipulator is

$$R=-EI_4\Big[\frac{3\epsilon}{(\ell_4-\ell_e)^3}+\frac{\partial^3 u_2}{\partial s^3}\Big]\bigg|_{z_4=\ell_4}. \tag{23}$$

If the bracing point does not move, the reaction force will not affect the flexible modes in the model. It will only effect the rigid body modes, that is, $\tau_1$ and $\tau_2$ would have increments given by

$$\Delta\tau_1=R(\ell_4+\ell_1c2) \tag{24}$$

$$\Delta\tau_2=R\ell_4. \tag{25}$$

Considering the reaction force on the bracing foot with the incremental torques given by Eqs. (24) and (25) and the regulator for the braced case described in appendix B, the actuator is turned on right after an impulse is applied on the dimension $\theta_1$. The time responses of $\theta_1$ and $\theta_2$ are shown in Figs. 10 and 11. Figure 12 shows the response of the reaction force, $R$. An initial static torque is required to cause a 37.5 $N$ shear force at the end of the upper link to prevent the bracing foot from detachment.

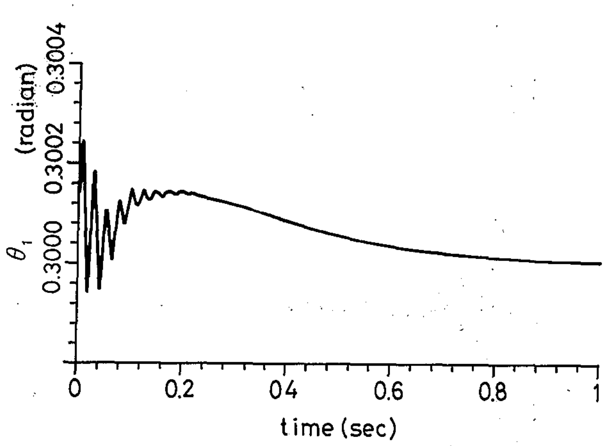


Fig. 10. Optimal control of lightweight bracing manipulator with considering end point bracing reaction.

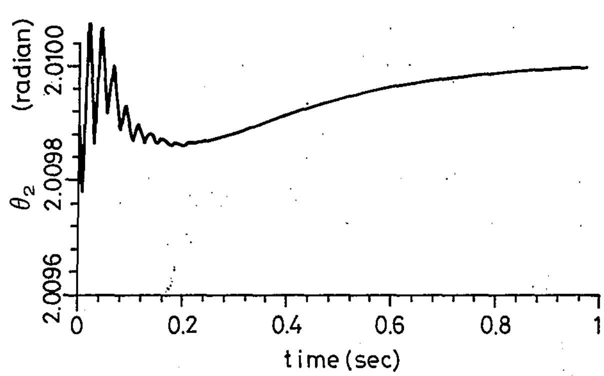


Fig. 11. Optimal control of lightweight bracing manipulator with considering end point bracing reaction.

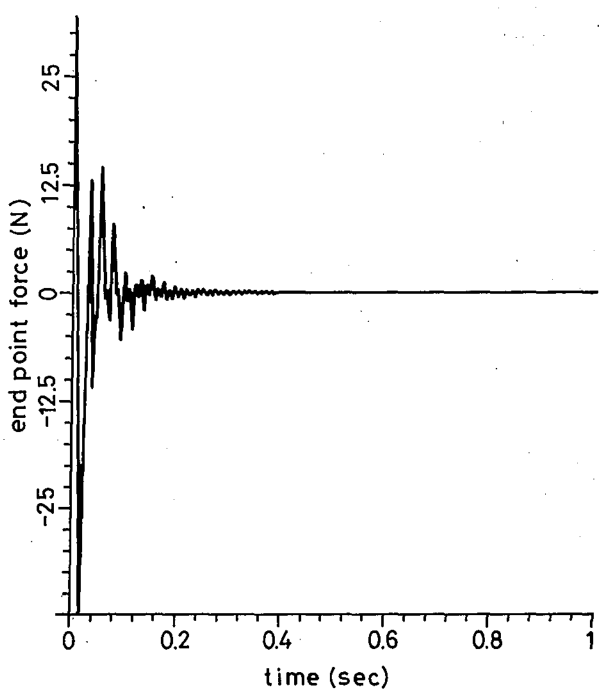


Fig. 12. Optimal control of lightweight bracing manipulator with considering end point bracing reaction.

## EFFECT OF NONLINEARITY

To simplify the analysis of designing a linear optimal regulator, all nonlinear terms were disregarded when linearizing the mathematical model. In the following, the effect of the nonlinearity will be considered by time response simulations. The lower link will be assumed rigid while keeping the upper link flexible. The double precision subroutine, DVERK, in IMSL is used in the nonlinear simulation. The time response of control torque are shown in Figs. 13 and 14.

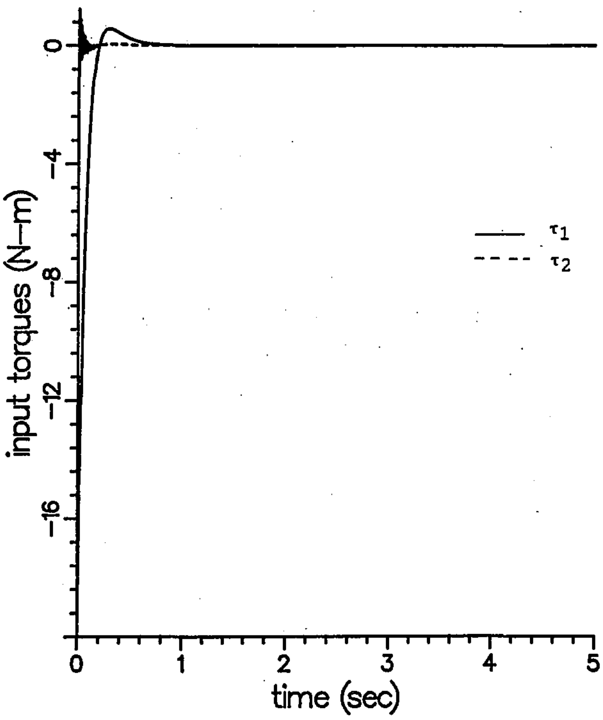


Fig. 13. Optimal control with linearized model, braced, higher prescribed relative stability controller.

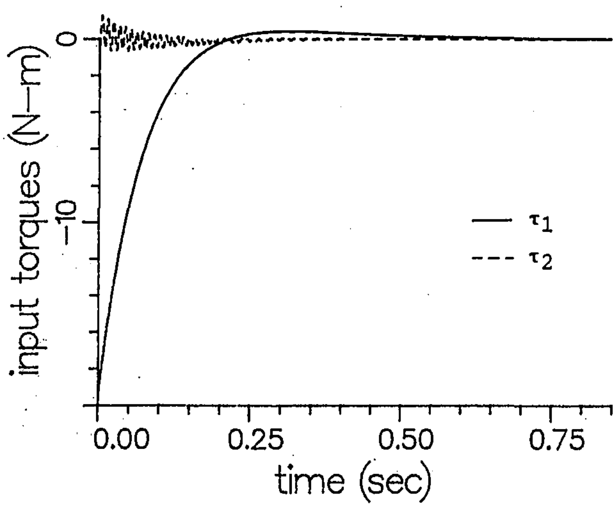


Fig. 14. Optimal control with nonlinearized model, braced higher prescribed relative stability controller.

## CONCLUSIONS

The bracing strategy is a milestone in the application of lightweight manipulators. It improves the stiffness of the lightweight manipulators. Using a developed mathematical model, a method of designing a linear regulator with prescribed relative stability has been outlined. The simulation results showed that the regulator has a good control effort to an impulse excitation. Both the nonlinear dynamics and the reaction force on the bracing foot have no adverse effect on the stability of the controlled system.

## REFERENCES

1. Alberts, T., G. Hastings, W. Book, and S. Dickerson, "Experiments in Optimal Control of a Flexible Arm with Passive Damping," *Fifth VPI and SU/AIAA Symp. Dyn. Control Large Struct.*, Blacksburg, VA (1985).
2. Anderson, B. O. D. and J. B. Moore, "Linear System Optimization with Prescribed Degree of Stability," *Proc. IEE*, Vol. 116, No. 12, pp. 2083-2087 (1969).
3. Armstrong, E. S., "ORACLS-A System for Linear-Quadratic-Gaussian Control Law Design," *NASA Technical Paper* 1106 (1978).
4. Asada, H. and H. West, "A Method for the Control of Robot Arm Constrained by Contact with the Environment," *Proc. 1985 American Control Conf.*, Boston (1985).
5. Balas, M. J., "Feedback Control of Flexible System," *IEEE Trans. Autom. Control*, Vol. AC-23, No. 4, pp. 673-679 (1987).
6. Book, W. J., "Modeling, Design and Control of Flexible Manipulator Arm," Ph. D. Dissertation, Department of Mechanical Engineering, M. I. T. Cambridge, Mass. (1974).
7. Book, W. J. and M. Majette, "Controller Design for Flexible Distributed Parameter Mechanical Arm Via Combined State Space and Frequency Domain Techniques," *J. Dyn. Syst. Meas. Control Trans. ASME*, Vol. 105, pp. 245-254 (1983).
8. Book, W. J., S. Le, and V. Sangveraphunsiri, "The Bracing Strategy of Robot Operation," *Symp. Theory and Practice of Robots and Manipulators*, Udine, Italy, pp. 139-145 (1984).
9. Chung, Y. C., S. S. Lu, and W. J. Book, "Modeling of Lightweight Bracing Manipulator," *10th Natl. Conf. Theor. Appl. Mech. STAM*, R. O. C., Kaohshung, pp. 177-191 (1986).
10. Hastings, G. and W. Book, "Experiments in the Control of a Flexible Manipulator," *ROBOTS 9 Exposition and Conference*, Detroit, MI (1985).

11. Ho, J. Y. L., "Direct Path Method for Flexible Multibody Spacecraft Dynamics," *J. Spacecraft*, Vol. 14, No. 2, pp. 102-110 (1977).
12. Holden, R. L., "A Braced End Effector for a Flexible Robot Manipulator," MS Thesis, School of Mechanical Engineering, Georgia Institute of Technology, Atlanta, Georgia (1985).
13. Kane, T. R. and D. A. Levinson, "DYNAMICS: Theory and Applications," McGraw-Hill, New York, N. Y. (1985).
14. Lakota, N. Y., Y. U. Rakhmakov, and V. N. Shvedov, "Trajectory C of An Elastic Manipulator," *Eng. Cybern*, Vol, 18, No. 2, pp. 45-52 (1980).
15. Wilson, T. R., "The Design and Construction of a Flexible Manipulator," MS Thesis, School of Mechanical Engineering, Georgia Institute of Technology (1985).

## APPENDIX A
### Data of Lightweight Bracing Manipulator

| | |
|---|---|
| stiffness of lower link | $EI_1=241{,}957$ N-m$^2$ |
| (Aluminum tube, outside dia. 141.3 mm, inside dia. 134.49 mm) | |
| stiffness of upper link | $EI_4=113{,}720$ N-m$^2$ |
| (Aluminum tube, outside dia. 114.3 mm, inside dia. 108.2 mm) | |
| stiffness of actuating link | $EI_3=20{,}992$ N-m$^2$ |
| (Aluminum column, outside width 101.6 mm, inside width 92.25 mm, outside height 44.45 mm, inner height 38.1 mm) | |
| the length of lower link | $\ell_1=3.048$ m (10 ft) |
| the length of connecting link | $\ell_2=0.4662$ m |
| the length of actuating link | $\ell_3=3.048$ m (actual 2.2 m) |
| the length of upper link | $\ell_4=3.958$ m |
| the lengtht of rigid part of upper link | $\ell_e=0.502$ m |
| the position length of small manipulator | $\ell_s=3.048$ m |
| mass per unit length of | |
| lower link | $\rho_1=3.9817$ kg/m |
| connecting link | $\rho_2=2.5$ kg/m |
| actuating link | $\rho_3=2.6545$ kg/m |
| rigid section of upper link | $\rho_e=6.58$ kg/m |
| flexible section of upper link | $\rho_f=2.893$ kg/m |
| the lumped mass at the end of lower link | $m_j=2$ kg |
| mass of small manipulator | $m_s=25$ kg |
| total mass of | |
| lower link | $m_1=12.136$ kg |
| connecting link | $m_2=1.1655$ kg |
| actuating link | $m_3=8.0909$ kg |
| upper link | $m_4=13.284$ kg |
| the position length of center of gravity of | |
| lower link | $r_1=1.524$ m |
| connecting link | $r_2=0.2332$ m |
| actuating link | $r_3=1.524$ m |
| upper link | $r_4=1.7903$ m |

## APPENDIX B
### Matrices and Closed Loop Eigenvalues in Optimal Control

$\boldsymbol{R}$: $\boldsymbol{I}$ (2×2)

$$
\boldsymbol{Q}=\left(\begin{array}{c|cccccc}
\boldsymbol{I} & & & O & & & \\
\hline
 & 10^5 & & & & & \\
 & & 10^3 & & & & \\
O & & & 10^5 & & & \\
 & & & & 10^3 & & \\
 & & & & & 10^5 & \\
 & & & & & & 10^5
\end{array}\right).
$$

**Non-braced case**

$$
\boldsymbol{F}=\begin{bmatrix}
3{,}995 & -4{,}875.96 & -9{,}221 & -36{,}291 & 180{,}988 & 7{,}321 & 1{,}917 & -1{,}473 & 942.4 & 309.98 & 6{,}018 & 2{,}481 \\
-25{,}815 & 40{,}782 & 11{,}726 & 25{,}503 & 3{,}358 & 10{,}113 & -1{,}149.5 & 1{,}233 & 1{,}014 & 334 & 1{,}123 & 3{,}356
\end{bmatrix}
$$

closed loop eigenvalues

$(-2{,}220+0j)(-718+0j)(-55+487j)(-47+230j)(-64+177j)$

$(-6.1+1.8j)(-6.2+1.03j)$

**Braced case**

$$
\boldsymbol{F}=\begin{bmatrix}
21{,}912 & -3{,}512.5 & -22{,}742.3 & -61{,}223.2 & 17{,}224.66 & 5{,}816.3 & 2{,}081 & -1{,}773.4 & 480.24 & 475.8 & 5{,}750.8 & 2{,}003.39 \\
6{,}685.7 & 62{,}141 & 24.110.17 & 24{,}503.93 & 5{,}473.56 & 10{,}923.8 & -866 & -940.67 & 630.72 & 656.9 & 1{,}757.2 & 3{,}567.2
\end{bmatrix}
$$

closed loop eigenvalues

$(-2{,}210.96+0j)(-758.6+0j)(-6.725+661.53j)(-26.74+452j)$

$(-50.15+239j)(-6.03+1.825j)(-6.196+0.931734j)$

Discussions of this paper may appear in the discussion section of a future issue. All discussions should be submitted to the Editor-in-Chief.

***Manuscript Received: November 8, 1986;***
***Revision Received: February 6, 1987;***
***Accepted: February 11, 1987.***